FATIGUE STRENGTH OF WELDED JOINTS OF 50E STEEL

J.M. FERREIRA*, C.M. BRANCO**

Experimental results were obtained in tension at R=0 and in bending for R=0 and 0.4. Semi-elliptical cracks were analysed at the weld toe and crack growth was monitored both at the surface and at the deepest point. Fatigue crack marking and potential drop was used. Good agreement was obtained between the experimental crack aspect ratios (a/c against a/B along the plate thickness) and the theoretical predictions obtained by one model derived by the authors.

The model computes fatigue crack growth rate using a Paris type law with m and C values experimentally obtained. The stress intensity equations were deducted with finite element techniques using 2D isoparametric model. Crack growth rate was computed both at the crack surface and at the deepest point.Good agreement was obtained bearing in mind the nature of the model.

INTRODUCTION

Fatigue behaviour of welded joints is influenced by many parameters specially the geometry of the weld and plate. Previous work carried out by Maddox (1) and Ferreira and Branco (2-4) identified the more important geometric variables of the fatigue behaviour of welded joints. The results have shown that the ratio ℓ/B (leg to leg distance over main plate thickness B), the main plate thickness and the radius of curvature at the weld toe, ρ are the key parameters of the fatigue strength of fillet welded joints.

In (2) and (3) some of the theoretical predictions of fatigue life were checked against experimental data obtained by the authors. Bearing in mind the influence of thickness and other geometrical parameters on the fatigue behaviour of welded joints it was decided to initiate a detailed investigation on this topic. In (4) an extensive set of results of the research is presented. S-N curves were obtained in T and cruciform non-load carrying joints with low to intermediate thickness values (4 to 20mm). Bending and tension loadings were considered for comparative purposes. The results in the low thickness range, specially those obtained in bending, have shown fatigue strength values lying considerably above the fatigue design curves in the codes. The main practical conclusion of the

*Department of Mechanical Engineering, University of Coimbra, 3000 COIMBRA - PORTUGAL.

**CEMUL, Lisbon University of Technology, 1096 LISBON CODEX - PORTUGAL

work is that the use of these design curves may lead to very conservative designs in thin sections commonly used in frames, chassis and thin attachments.

In this paper experimental fatigue life results and crack growth data are presented concerning bending. The objective of the research is to verify the crack growth assumptions used in the previous analysis and test the accuracy of the solutions. The low carbon steel BS50E chosen for this work is of the same grade as that used before so that comparison of data could be possible.

EXPERIMENTAL

The low carbon steel 50E was supplied in plates with nominal thickness of 12mm. The chemical composition and mechanical properties are given in the following table:

C	S_i	M_n	N_i	C_r	M_o	V	C_u	N_b	T_i	Al
0.16	0.3	0.35	0.02	0.03	0.01	0.002	0.04	0.04	0.002	0.034

Yield stress, σ_{ys} = 381 MPa; σ_{UTS} = 548 MPa; ε_r = 20%

Crack propagation data was obtained in base metal and in bending in specimens with the same overall dimensions as the welded specimens. The fatigue tests were performed in air at room temperature at a loading frequency of 25Hz. Two stress ratio values were used, R=0.05 and 0.4 and two types of crack starters were used; semi-elliptical and through notches with the same a/B ratio. The crack length a at the specimen top surface was measured with a travelling microscope and the crack depth was monitored with an AC potential drop system.

FATIGUE LIFE PREDICTION

The fatigue life prediction was done assuming crack propagation from an initial flaw size of 0.15mm with a semi-circular shape. The crack was assumed to grow from this initial size till 60% of the plate thickness. The Paris law was used in the computation with all the following assumptions:

i) experimental values of m and C_A were used for the crack propagation in the depth direction;

ii) The value of C_B for the crack length a direction was $C_B = 0.9^m C_A$;

iii) K_A at the deepest point, A, was calculated in the depth direction and given by M_K factor previously obtained by the authors (2-4) and who takes into account the effect of weld geometry, multiplied by the K base solution of Raju and Newman (5) also for the deepest point of the crack;

iv) K_B at the surface was given by the Raju K base solution at the surface times the M_K factor for a crack depth of 0.15mm.

The M_K solutions were obtained before using the weigth function method with a 2D isoparametric FE program (2-4).

RESULTS AND DISCUSSION

Table 1 gives the m and C values in bending (mm/cycle; $Nmm^{-3/2}$). The plots da/dN; ΔK were obtained with the procedure outlined in the ASTM specification (6). The K values were obtained with the Murakami equation (7) for through cracks in a bar loaded in bending.

TABLE 1 - Values of m and C for 50E steel

Specimen type and crack	R	m	C
Cantilever bending; through crack	0	3.5	$9.0x10^{-15}$
Cantilever bending variable cross section; through crack	0	3.5	$3.2x10^{-15}$
Cantilever bending variable cross section; through crack	0	3.5	$2.9x10^{-13}$
Cantilever bending variable cross section; semi-elliptical crack	0.4	3	$2.5x10^{-15}$
Cantilever bending variable cross section; dc/dN	0	3.5	$2.5x10^{-15}$

This data gives $C_B = C_A x\ (0.95)^{3.5}$

Figure 1 shows the influence of R on da/dN for through cracks. For straight cracks the value of m decreases and C increases when R changes from 0 to 0.4. The fatigue threshold ΔK_{Lf} decreases with R (Figure 1). For semi-elliptical cracks there is only a small increase of da/dN with R.

The da/dN, ΔK plots for R = 0 and both for through and semi-elliptical cracks are in Figure 2. The results for semi-elliptical cracks are very close to those for through cracks. However for the through cracks, crack growth rate is higher in the specimens with a constant cross section in comparison with the specimens with variable cross section.

All the bending data fits into the scatter band previously obtained in CT specimens with thickness ranging from 4 to 22mm where m=3 and C between $4,5x10^{-14}$ and $1.9x10^{-13}$.

Figure 3 shows the crack shape data (a/c against a/B). The experimental points obtained by the potential drop method can be compared with the theoretical solution mentioned before without the M_k factor. The values of m=3 and $C_A = 1.9x10^{-13}$ refering to the upper curve of the scatter band of the CT specimens were used. There is a good agreement between the experimental results and the

theoretical predictions. Hence these values of m and C and the computational method are the more suitable for the fatigue life prediction in the T and cruciform joints made of this material. A confirmation is presented in Figures 4 to 6 showing the experimental data obtained in cruciform joints in tension (Figure 4) and in T joints in bending (Figures 5 and 6) plotted against the computed fatigue curves obtained in (4). The agreement between the experimental results and the fatigue prediction is good in the small thickness range ($B < 12mm$) and for a radius of curvature at the weld toe close to 1mm, the most probable value of radius found in this type of welded joints (4).

CONCLUSIONS

1- Fatigue crack growth rate is similar for semi-elliptical and through cracks.

2 - The stress ratio R has a more pronounced effect in through cracks than for semi-elliptical cracks.

3 - For R=0 the da/dN; ΔK results are within the scatter band obtained in the CT specimens for the thickness range 4 to 22mm.

4 - In welded joints the best agreement between the experimental fatigue results and the theoretical prediction are with the Raju solution and M_K factor and using the values of m and C obtained experimentally in both crack propagation directions in specimens of base material with the same nominal thickness and subjected to the same loading mode.

REFERENCES

(1) - Maddox, S.J., "Fatigue life prediction methods in welded joints", Proc. NATO ASI Advances in Fatigue Science and Technology, Ed. Kluwer Academic Press, Eds. C. Moura Branco, L. Guerra Rosa, 1989, pp. 569-585.

(2) - Ferreira, J.M. and Branco, C.M., "Influence of weld size and plate length in the fatigue strength of fillet welded joints", Fract. Mech. Tech. 9, 1988, pp. 23-32.

(3) - Ferreira, J.M. and Branco, C.M., Influence of the radius of curvature at the weld toe in the fatigue strength of fillet welded joints", Int. J. Fatigue, 2, 1989, pp. 29-36.

(4) - Ferreira, J.M. and Branco, C.M., "Fatigue analysis and prediction in fillet welded joints in the low thickness range", Fat.Fract.Eng.Mater.Struct., 1990.

(5) - Newman, J.C and Raju, I.S., "Stress intensity factor equations for cracks in three dimensional finite bodies subjected to tension and bending loads", NASA TM 85793, Langley Research Center, Virginia, U.S.A., 1984.

(6) - ASTM E647-81, "Constant load amplitude fatigue crack growth rates above 10^{-8} m/cycle", Annual book of ASTM standards, U.S.A., 1981.

(7) - Murakami, Y., "Analysis of mixed mode stress intensity factors by body force methods", Num.Meth. in Fract.Mech., D.R.I. Owen and A.R. Luxmore, Ed. Pineridge Press, U.K., 1980.

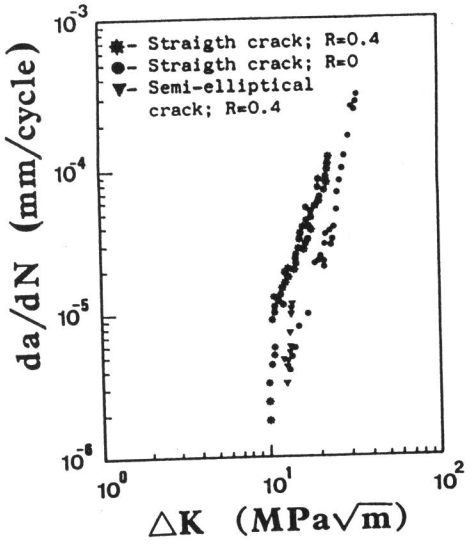

Figure 1 - da/dN against ΔK. Influence of R and type of specimen. 50E steel. B = 12mm.

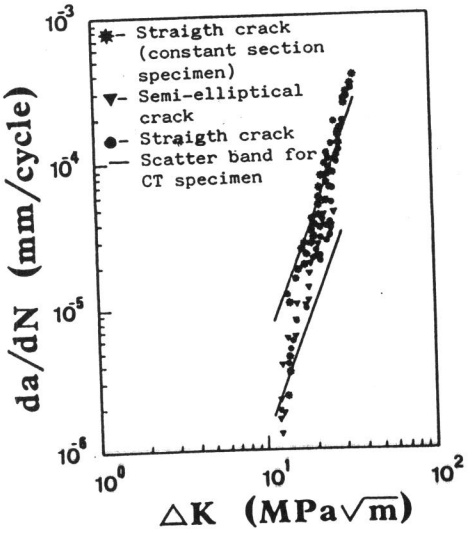

Figure 2 - da/dN against ΔK. R = 0. Bending and tension. 50E steel. B = 12mm.

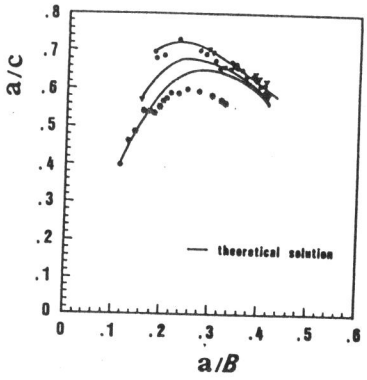

Figure 3 - a/c vs. a/B. B=12mm. 50E steel. Bending.

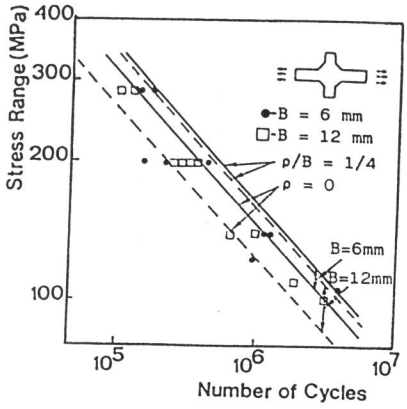

Figure 4 - S-N curves. B=6 and 12mm. 50E steel. Bending

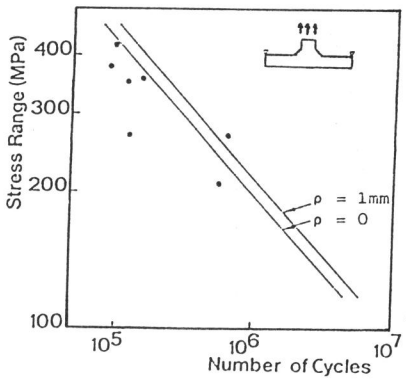

Figure 5 - S-N curves. B=6mm 3PB. 50E steel.

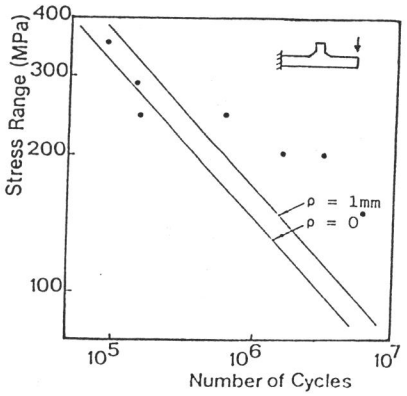

Figure 6 - S-N curves. B=12mm. Cantilever bending. 50E steel.